Journal of Polymer Research **11:** 75–83, 2004.

Morphological, Thermal, Barrier and Mechanical Properties of LDPE/EVOH Blends in Extruded Blown Films

Chi-Hsien Huang[1], Jiann-Shing Wu[1,*], Chun-Chin Huang[2] and Li-Shin Lin[3]
[1]*Department of Applied Chemistry, National Chiao Tung University, 1001 Ta Hsueh Road, Hsinchu 300, Taiwan, R.O.C.*
[2]*Department of Mold and Die Engineering, National Kaohsiung University of Applied Science, Kaohsiung 807, Taiwan, R.O.C.*
[3]*Chang Chun Petrochemical Co., Ltd., Miaoli 360, Taiwan, R.O.C.*
*(*Author for correspondence; E-mail: jswu@cc.nctu.edu.tw)*

Received 26 August 2003; accepted in revised form 22 October 2003

Key words: blending, blown film, EVOH, LDPE-g-MAH, oxygen barrier

Abstract

We have investigated the morphological, thermal, barrier, and mechanical properties of low-density polyethylene/ethylene–vinyl alcohol blend (LDPE/EVOH; 85/15 wt%) in highly and biaxially oriented blown films. Maleic anhydride-grafted linear low-density polyethylene (LDPE-g-MAH) in various concentrations (from 0 to 10 phr) was used as the compatibilizer for the immiscible system. Thermal analysis of the blend films shows that their melting temperatures, crystallization temperatures, and heats of fusion stay almost constant upon varying the amount of compatibilizer. The addition of the compatibilizer did not adversely affect the inherent properties of the blends, especially their barrier properties, through constraint effects of the grafted EVOH (EVOH-g-LD). The heat of fusion of EVOH obtained during the first heating is much higher than that of the second as a result of stress-induced crystallization during the blown film process. Oxygen permeation measurements show that the oxygen barrier properties of both highly and biaxially oriented blown films decrease upon increasing the amount of compatibilizer, although morphological analysis showed that the blends exhibit better laminar dispersion of the EVOH phase in the LDPE matrix when LDPE-g-MAH is added. The increase in oxygen permeability results from the presence of microvoids at the interface between the two phases during the process. Mechanical measurements showed that there exists an optimal amount of LDPE-g-MAH for maximizing both the tensile and tear properties in both the machine and transverse directions.

Introduction

Plastic materials with good gas- and solvent-barrier properties offer a variety of advantages over metals and glasses for use in applications such as packaging films and containers. The most important requirement for the use of plastics in food packaging films is their impermeability to gases (i.e., the barrier property). Mechanical properties, especially tensile and tear properties, should also meet final product specifications. No single polymeric material, however, can offer all of the required properties and, therefore, a combination of polymers is generally employed.

Polyolefins, such as polyethylene (PE) and polypropylene (PP), are the most widely used resins applied as films for packaging because of their good mechanical and barrier properties towards moisture. Ethylene–vinyl alcohol copolymer (EVOH) has excellent gas-barrier properties and resistance to oil and organic solvents [1–4]. It is very sensitive to moisture, however, and loses its gas-barrier properties at high relative humidity because water acts as a plasticizer, weakening the hydrogen bonding between the polymer molecules [5–8]. Thus, in modern food packaging technology, it is common to coextrude multilayer films that consist of distinct layers that act as barriers to both moisture and gas. Coextruded multilayer films have been made by processing cap materials (such as PE or PP), tie resins, and the center barrier resins [such as EVOH or PA (polyamide)] through their respective extruders and a feedblock, and then through a die to give typical five-layer films [9]. This technology, however, comes at a high cost and requires a complex degree of control, and the final product is not recyclable. A current alternative approach, employing polymer blends, appears to be beneficial for designing materials from a combination of a barrier material (EVOH) and a lower-cost matrix material (PE or PP). The blend processing can occur in a single-step operation and offers process versatility and low product cost [10, 11]. The ultimate behavior of the polymer blend depends largely on the morphology of the blend. Previous studies have established that the formation of a laminar morphology in a polymer blend increases the tortuous path, which improves the barrier properties [12–14]. The morphology of a polymer blend is determined by many factors, such as the interfacial tension, the blend composition, the viscosity ratio of the components, the blending sequence,

and the processing conditions, which include the temperature, residence time, flow history, shear stress, and draw ratio [12–19].

One of the most important methods for controlling the blend morphology is modifying the interface between the phases, by addition of a compatibilizer, to obtain greater compatibility [20, 21]. The compatibilizer may reduce the interfacial tension and, hence, increase the adhesion between phases and, as a result, allow a finer dispersion, a more stable morphology, and an improvement in mechanical [15, 22–27] and barrier properties [12–14]. The compatibilizer also affects the crystallization and melting behavior of the polymer blend [15, 28, 29].

Previous reports have described the preparation of samples of blend films that are relatively very thick – several hundreds of microns [15, 19, 30] – but, in most applications, films are usually required to have a thickness of about a hundred microns or less. In this paper, we report relatively thinner film blends fabricated by an extruded blown-film process, using conventional processing conditions to produce highly and biaxially oriented films. We investigated the effects that the compatibilizer has on the morphological, thermal, barrier, and mechanical properties of LDPE/EVOH blend films.

Experimental

Materials

Commercial grade low-density polyethylene [LDPE, 6030F, M. I. (g/10 min, 190 °C, 2.16 kg) = 0.27, density = 0.922 g/cm^3] was supplied by Formosa Plastic Corp. (Taiwan) in pellet form. The ethylene–vinyl alcohol copolymer was provided in pellet form [EVOH, F101A, ethylene content (mol%) = 32, M. I. (g/10 min, 190 °C, 2.16 kg) = 1.6, density = 1.19 g/cm^3] by Kuraray Co. (Japan). The compatibilizer, Modic-AP L502, was obtained from Mitsubishi Chemical Corp. (Japan). It is a low-density polyethylene-grafted maleic anhydride (LDPE-g-MAH).

Blend Film Preparation

In each blend, the weight ratio of LDPE to EVOH was 85:15, and the amount of the compatibilizer was 0, 0.5, 1, 2, 4, 6, 8 or 10 phr. All components were premixed by tumbling and then fed simultaneously into the single-screw extruder (diameter = 42 mm, L/D = 28) attached to the blown-film die (inner diameter = 76 mm; gap thickness = 1.2 mm). The temperature profiles for the three heating sections of the extruder barrel and die were set at 190, 210, 230, and 240 °C, and the screw speed was 45 rpm. Above the exit of the die, the blend films were inflated and cooled with air and stretched by a take-off device. The ratios of take-off (take-off linear rate/linear rate of extrusion) and blow-up (diameter of bubble/diameter of blown-film die) were 8 and 2.6, respectively, and the frost-line height was 40 cm. Because of its hygroscopic behavior, EVOH was dried carefully in a vacuum oven for 24 h at 60 °C before blending. For comparison, pure EVOH and LDPE films were prepared under the same processing conditions.

Morphological Analysis

We used two methods to obtain information on the different morphological behavior of the LDPE/EVOH blends upon the addition of LDPE-g-MAH. In the first method, specimens were prepared by fracturing the blend films cryogenically. The fracture surface was coated with a thin layer of gold and observed by scanning electron microscopy (SEM). In the second method, the blend films were placed between a pair of glass slides and treated in hot xylene, which resulted in selective dissolution of the LDPE matrix and separation of the EVOH dispersed phase. The separated EVOH domains were examined with an optical microscope (OM) so that we could determine the actual shape of the dispersed EVOH domains.

Thermal Analysis

Differential scanning calorimetry (DSC, TA instruments Q10) was used to study the melting temperature and crystallization of the blend films. In each heating cycle, the temperature was increased from 30 to 220 °C at a rate of 10 °/min, maintained at 220 °C for a period of 5 minutes, and then cooled to 40 °C at −2 °/min to erase the thermal history.

Permeability Measurements

The oxygen-permeability properties of blend films were measured using a Lyssy L-100-5000 Gas Permeability Tester, following the ASTM Standard Method D1434. The oxygen permeability of the blend films were measured at 23 °C with a relative humidity of 0%. The temperature of both the testers was controlled by a water bath. The detailed procedure of tester is summarized in [31].

Mechanical Measurements

The mechanical measurements, including tensile and tear properties, of the blend samples were performed using a tensile tester at room temperature, following the procedures described in ASTM D882 and D1938, respectively. For both measurements, at least ten samples were tested in both the machine and transverse directions.

Results and Discussion

Morphological Characterization

In this study, the compatibilizer (LDPE-g-MAH) was used to reduce the interfacial tension and, hence, to increase the adhesion between the two immiscible phases of LDPE and EVOH. Furthermore, it also prevents coalescence of the dispersed particles during the melt flow through a die after the dispersed domains have been crushed by the high shear stress induced by screw rotation in the extruder [20].

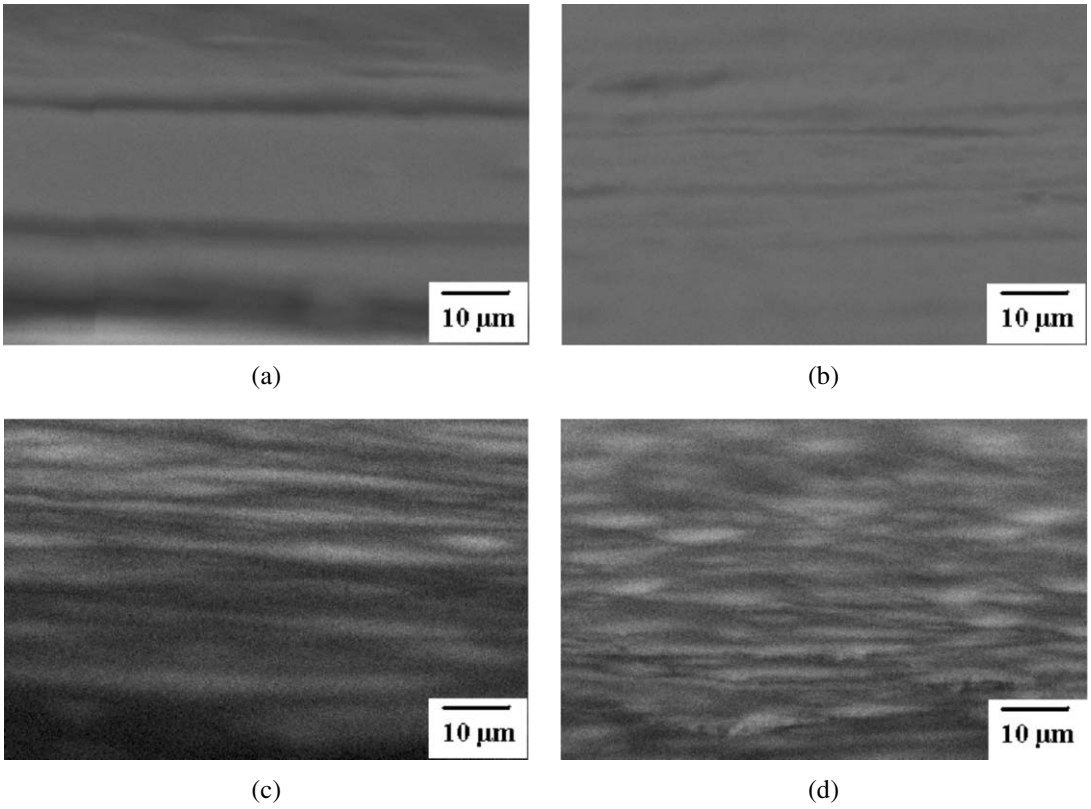

Figure 1. SEM micrographs of LDPE/EVOH blend films with various compatibilizer contents: (a) 0 phr; (b) 1 phr; (c) 4 phr and (d) 8 phr.

Figure 1 shows SEM images of the morphological changes across the film thickness of the LDPE/EVOH blend films prepared with varying amounts of compatibilizer (from 0 to 8 phr). We observe more and thinner EVOH layers (laminar-like structures) when the amount of compatibilizer was increased. Figure 2 shows the optical micrographs of the LDPE/EVOH blend films prepared with various amounts of compatibilizer (from 0 to 10 phr). We see that the dispersed EVOH domain deforms into fibrils in the LDPE matrix when the amount of compatibilizer is small. This effect is due to efficient transfer of shear stress from the LDPE matrix to the dispersed EVOH domain during extrusion and, subsequently, by the high drawing and cooling rates [16, 32]. As the amount of compatibilizer is increased, the shape of the dispersed EVOH domain changes gradually from fibrils to small spherulites. This change is due to the fact that the increasing amount of compatibilizer results in a decrease in the interfacial tension and leads to smaller EVOH domains; it is difficult to deform the small particles during the extrusion and subsequent drawing and blowing processes [33, 34].

Melting and Crystallization

Figures 3 and 4 show the first and second heating thermograms of LDPE/EVOH blend films having varying amounts of compatibilizer. The endothermic peak temperatures of both LDPE and EOVH are not changed significantly upon addition of the compatibilizer and remain almost constant during both heating cycles. In addition, these temperatures are roughly the same as those of the corresponding bulk polymers. The heat of fusion of LDPE remained constant upon the addition of the compatibilizer, but that of EVOH slightly increased and then remained constant when the amount of compatibilizer was greater than 4 phr. These results for LDPE are the same as those found by Lee and Kim [15], but our results for EVOH are somewhat different from their findings that the endothermic peak temperature and heat of fusion for EVOH decrease with increasing amounts compatibilizer as a result of constraint effects of the grafted EVOH in the dispersed EVOH phase. We observed no depression of either the melting temperature or the heat of fusion of EVOH. These results could be due to the existence of chemical bonds that form only at the surface of the EVOH domains, which is a situation that will not result in constraint effects of the grafted EVOH (EVOH-g-LD) or destruction of the inherent properties of EVOH.

Figure 5 displays the melting peak temperatures of LDPE/EVOH blend films during the first and second heating cycles. The melting peak temperatures of the first heating cycle were higher by ca. 1 °C than those of the second for both LDPE and EVOH at all amounts of compatibilizer. The temperature difference may be due to the different cooling rates between the blown-film process and the DSC cooling process. Since the cooling rate in the DSC program is much slower than that in the blown-film process, the polymer chains of both LDPE and EVOH can crystallize better, which leads to the higher melting temperatures.

Figure 6 displays a comparison between the heats of fusion of the first and second heating cycles. The heats of fusion of LDPE for both heating cycles are very close, but

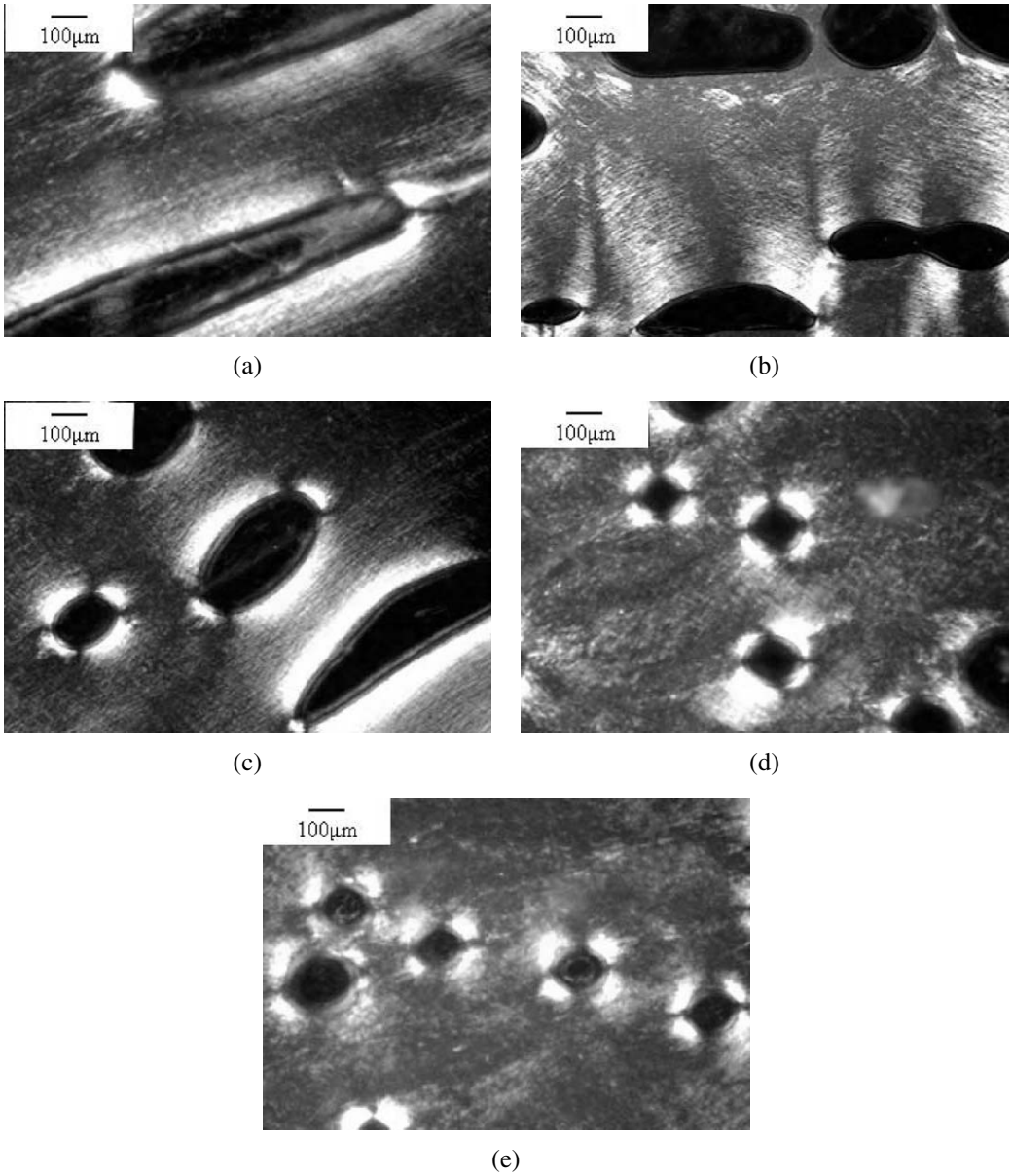

Figure 2. Optical micrographs of LDPE/EVOH blend films with various compatibilizer contents: (a) 0 phr; (b) 0.5 phr; (c) 1 phr; (d) 6 phr and (e) 10 phr.

the heat of fusion of EVOH for the first heating cycle is much higher than that of the second, which is an observation that we attribute to stress-induced crystallization resulting from stretching and molecular alignment (high and biaxial orientation) of the blown films during the blown-film process. This phenomenon explains why the heat of fusion of the uncompatibilized LDPE/EVOH blend films is slightly smaller than those of the compatibilized ones, as shown in Figures 3 and 4. The transfer of stress from the LDPE matrix to the dispersed EVOH domain in the uncompatibilized LDPE/EVOH blend is less than that of the compatibilized LDPE/EVOH blend during the extrusion and subsequently high drawing and blowing processes.

Figure 7 shows the cooling thermograms of LDPE/EVOH blend films having varying amounts of compatibilizer. The exothermic peak temperatures of both LDPE and EVOH do not change significantly upon addition of the compatibilizer and remain at almost a constant temperature during both the first and second heating cycles. Additionally, these temperatures are roughly equal to the values of the corresponding bulk polymers. The heats of crystallization also remain constant for both LDPE and EVOH, which is a situation that can be explained using the same reasoning we used in discussing Figures 3 and 4.

Oxygen Barrier Properties

Figure 8 displays the effect of compatibilizer content on the oxygen permeability of LDPE/EVOH blend films, which are highly and biaxially oriented (blow-up ratio: 2.6; take-off ratio: 8). As indicated, the oxygen permeability is initially reduced upon the addition of compatibilizer. As the amount of compatibilizer increases, the oxygen permeability also increases slightly. There existed a better barrier oxygen property of blend films than that of pure LDPE as shown in Figure 8.

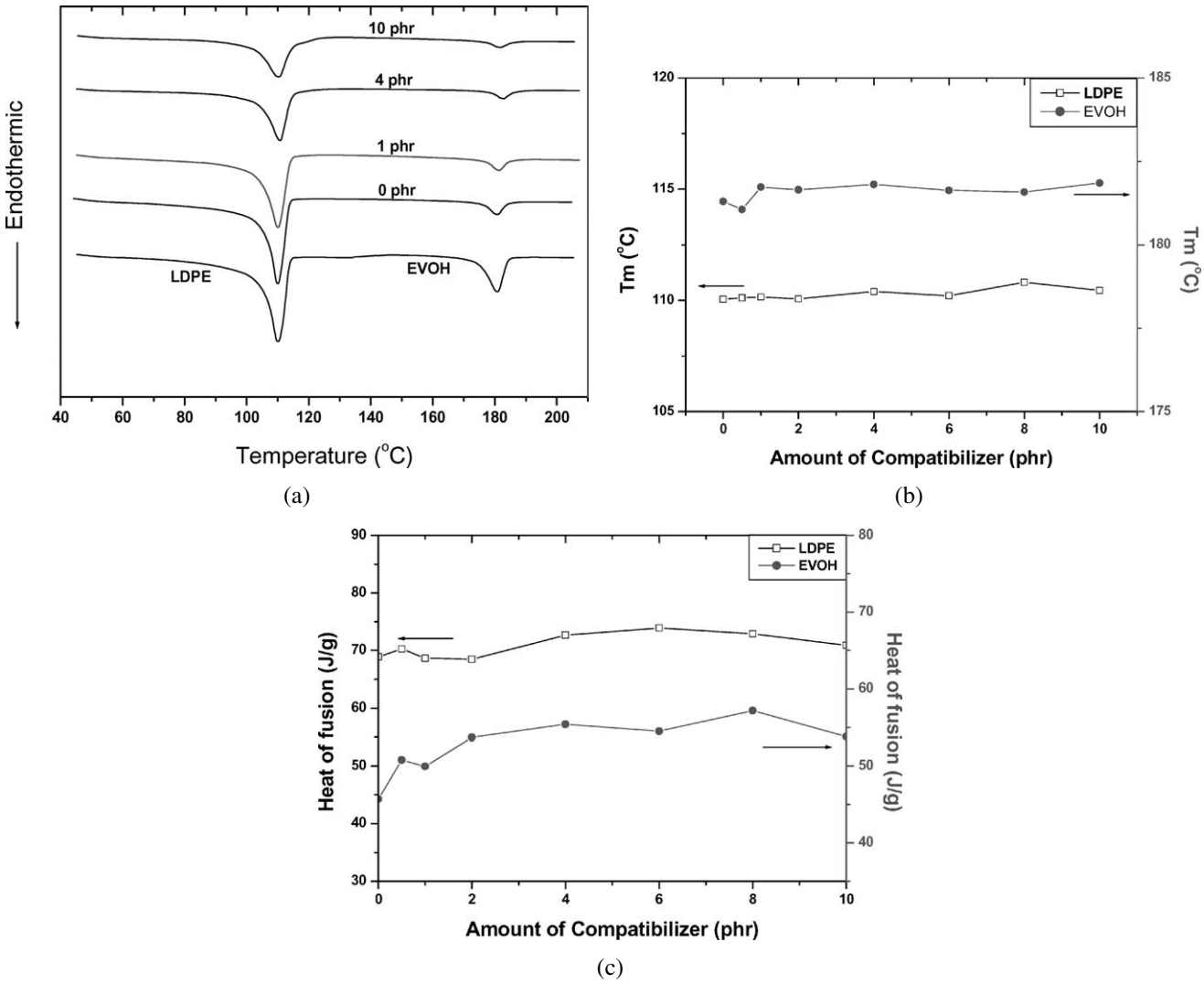

Figure 3. The DSC first heating thermograms, melting peak temperatures (T_m) and heat of fusion of LDPE/EVOH blend films with various compatibilizer contents: (a) DSC heating thermograms; (b) melting peak temperature (T_m); (c) heat of fusion.

The results of oxygen permeability measurements of the compatibilized LDPE/EVOH blend films fabricated by high- and biaxial-oriented blown-film processes differ somewhat from those of PP/EVOH [19]. For PP/EVOH, there exists an optimal amount of compatibilizer for obtaining maximized barrier properties in well-developed laminar structures of blend films that were fabricated by the biaxially stretched cast-film process with a draw ratio of 3.5 × 3.5 at 160 °C. In our current study, although the blend films have well-developed laminar structures upon adding the compatibilizer, as shown in Figures 1 and 2, their oxygen permeabilities increase slightly as the amount of compatibilizer increases. This effect may be due to the poor miscibility between LDPE-g-MAH and LDPE/EVOH blend films fabricated by the blown-film process (highly and biaxially stretched), which results in the formation of microvoids during cooling because of the large difference in crystallization temperatures, as shown in Figure 7. During cooling in the blown-film process, the dispersed EVOH domain crystallizes earlier than does LDPE and becomes a heterogeneity in the LDPE matrix, which causes the stress of the matrix, induced by the high and biaxial orientation, to transfer to the EVOH domains by compatibilizer difficultly and results in a concentration of stress at the interface of the two phases, which results in microvoids forming there. Although the EVOH domain yields more and thinner dispersed phases as the amount of compatibilizer increases, resulting in an increase in the contour length of the interface between the two phases as shown in Figure 2, this phenomenon increases the likelihood of microvoid formation during cooling and increases the oxygen permeability slightly.

In this study, uncompatibilized blend films were observed having poor barrier properties because oxygen molecules can diffuse easily through the microvoids formed at the interface between the two immiscible phases during the biaxially oriented blown film process.

Mechanical Properties

Tensile Properties

The tensile properties of our blend films in both the machine direction (MD) and the transverse direction (TD) are displayed in Figures 9 and 10. In Figure 9, we see that

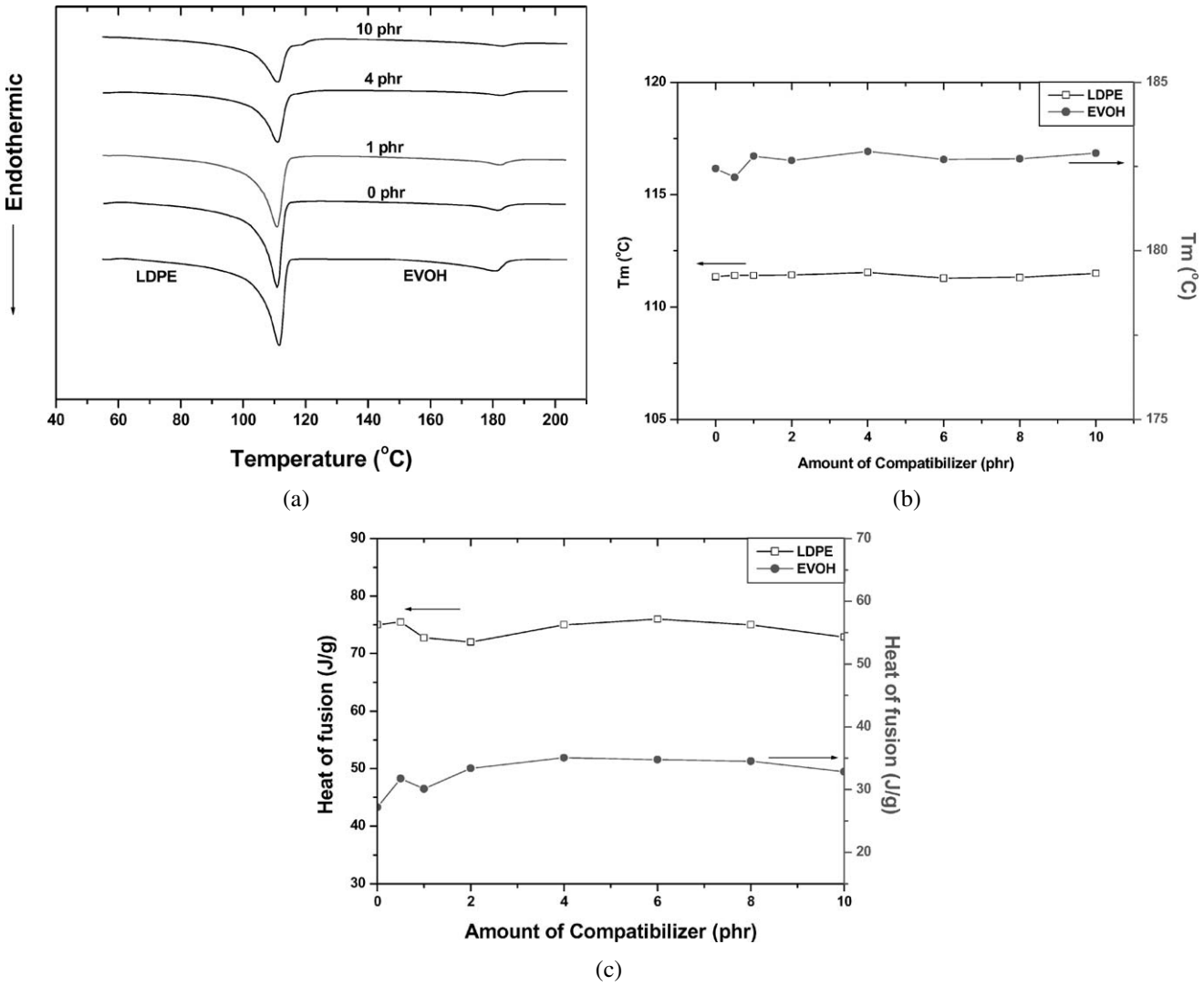

Figure 4. The DSC second heating thermograms, melting peak temperature and heat of fusion of LDPE/EVOH blend films with various compatibilizer contents: (a) DSC heating thermograms; (b) melting peak temperature (T_m); (c) heat of fusion.

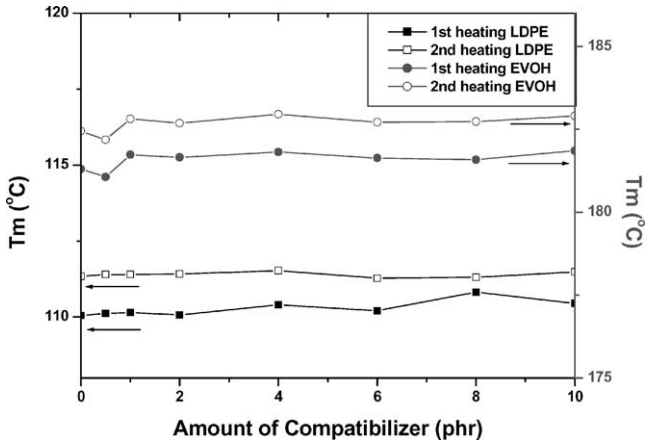

Figure 5. Melting peak temperatures of first and second heating of LDPE/EVOH blend films with various compatibilizer contents.

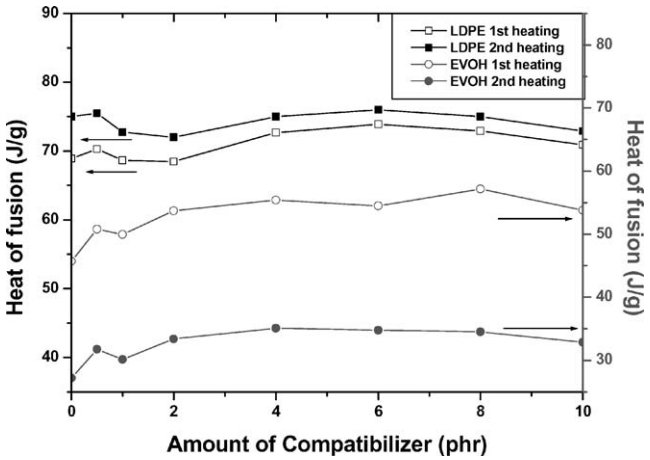

Figure 6. Heat of fusions of first and second heating of LDPE/EVOH blend films with various compatibilizer contents.

the MD tensile strength at the break of the blend films initially increases with increasing compatibilizer content of up to 1 phr, and then decreases and stays constant. Moreover, we have found that the addition of a compatibilizer to be a method for improving the mechanical properties of immiscible blends, and that the optimal compatibilizer content for maximizing MD tensile strength at the break is also a result

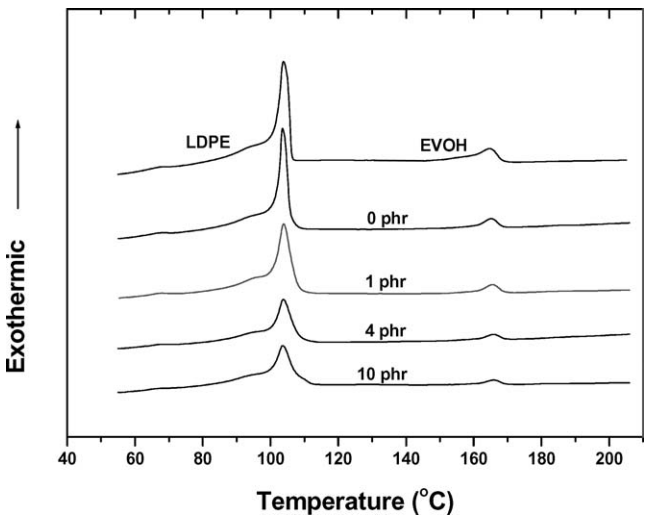

(a)

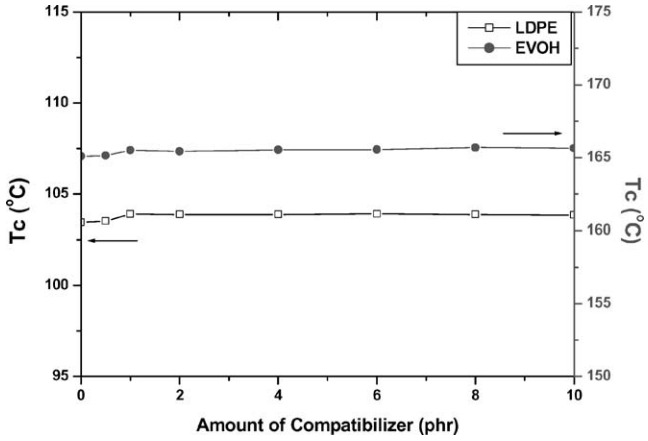

(b)

Figure 7. The DSC cooling thermograms and crystallization peak temperature (T_c) of LDPE/EVOH blend films with various compatibilizer contents (cooling rate = 2 °C/min): (a) DSC cooling thermograms; (b) crystallization peak temperature (T_c).

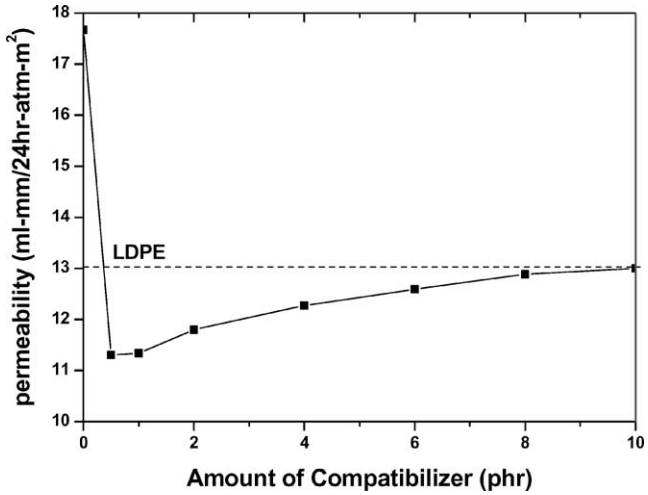

Figure 8. Oxygen permeability of LDPE/EVOH blend films with various compatibilizer contents. Dash line represents the oxygen permeability of LDPE.

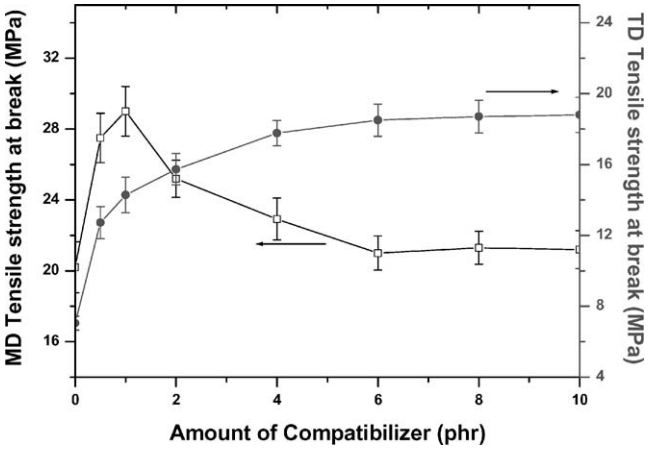

Figure 9. Tensile strength at break of LDPE/EVOH blend films with various compatibilizer contents for both MD (machine direction) and TD (transverse direction).

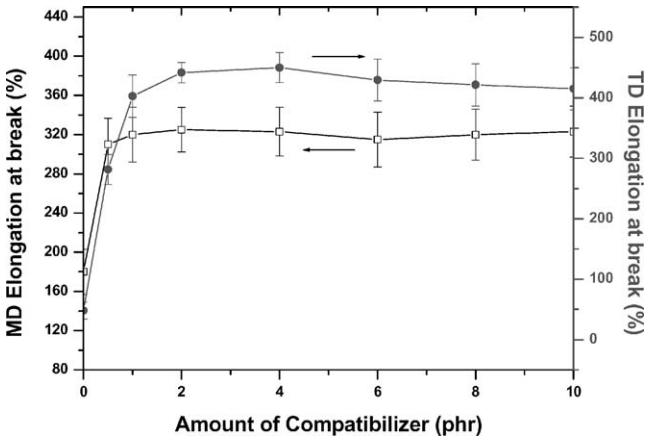

Figure 10. Elongation at break of LDPE/EVOH blend films with various compatibilizer contents for both MD (machine direction) and TD (transverse direction).

of the morphology as shown in Figure 2. In Figure 2(c), the shapes of the dispersed EVOH domains are elongated fibrils aligned to the MD and the strength of the pure EVOH film is much higher than that of LDPE (Table I). Thus, we believe that systems of LDPE/EVOH blends having low amounts of compatibilizer behave like fibril-reinforced composites [25, 35, 36]. As the shape of the dispersed EVOH domains changes from fibrils to spherulites, as shown in Figure 2, the effect of the fibril reinforcement disappears and the tensile strength decreases. The TD tensile strength at break of the blend films increases upon increasing the compatibilizer content. Increasing the compatibilizer content results in reduction of the dispersed EVOH domain size, which leads to less stress concentrating at the interface between the dispersed phase and the matrix phase and results in increasing tensile strength in the TD. The elongation at break in the MD and TD initially increases with increasing compatibilizer content and then stays constant, as shown in Figure 10, which we attribute to enhancement of the interfacial adhesion between the LDPE and EVOH phases.

Table 1. Tensile properties of pure LDPE and EVOH films for both MD (machine direction) and TD (transverse direction) (ASTM D882)

Material	Tensile strength at break (MPa) MD	Tensile strength at break (MPa) TD	Elongation at break (%) MD	Elongation at break (%) TD
LDPE	28	29	550	650
EVOH	60	55	270	250

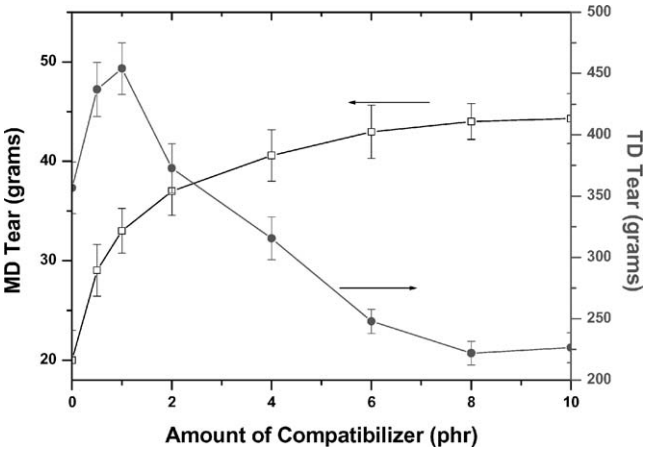

Figure 11. Tear propagation resistance of LDPE/EVOH blend films with various compatibilizer contents for both MD (machine direction) and TD (transverse direction).

Tear Properties

Figure 11 displays the tear propagation strength in both the MD and TD. The MD tear propagation strength varies with the compatibilizer content, as does the TD tensile strength. On the other hand, the TD tear propagation strength varies with the amount of compatibilizer, as does that MD tensile strength. As a result, the failure mechanism of tear propagation in the MD and TD are like those of the tensile failure in the TD and MD, respectively. The TD tear strength has a much higher value than that of the MD, which is a phenomenon that is due to the high degree of orientation of the molecules in the MD.

Conclusions

In this study, LDPE/EVOH blend films, highly and biaxially oriented, were fabricated successfully by a blown-film process. By investigating the morphological, thermal, barrier, and mechanical properties of LDPE/EVOH blend films with respect to their compatibilizer content, we reach the following conclusions: (1) In the LDPE/EVOH binary system, the EVOH domains have fibril-like structures at low amounts of compatibilizer and are spherulite-like at high levels. When the amount of compatibilizer increases, the EVOH domains yield more and thinner EVOH layers, which result from lower interfacial tension. (2) The melting and crystallization processes do not change significantly with the addition of the compatibilizer because there is little or no constraint effect of the grafted EVOH (EVOH-g-LD). (3) There is a large difference in the heat of fusion between the first and second heating cycles. During the blown-film process, high and biaxial orientation leads to stress-induced crystallization. The processing and thermal history is faded during the DSC isothermal program prior to the second heating cycle, which results in a lower heat of fusion than in the first. There is also a difference in the cooling rates of the blown-film process and the DSC program. The cooling rate in the DSC program (2 °/min) is much slower than that in the blown-film process, and so the polymer chains of both LDPE and EVOH can crystallize more perfectly, which leads to higher melting temperatures. (4) Oxygen permeability of the LDPE/EVOH blend films is reduced slightly upon increasing the amount of compatibilizer as a result of the presence of microvoids between the two phases. The microvoids, which form during cooling in the blown-film process, result in more gas being able to pass through the LDPE/EVOH blend films and, hence, they increase the oxygen permeability. (5) We found that there is an optimal level of compatibilizer content (1 phr) for maximizing the MD tensile strength and elongation. On the other hand, increasing the amount of compatibilizer results in an increase in the TD tensile strength and elongation. The trend of tear strength with respect to the amounts of compatibilizer is similar to that observed for the tensile strength.

References

1. R. H. Foster, *Packaging*, **32**, 70 (1987).
2. T. Iwanami and Y. Hirai, *Tappi J.*, **66**, 1404 (1983).
3. J. M. Lagaron, A. K. Powell and G. Bonner, *Polym. Test.*, **20**, 569 (2001).
4. H. U. Beckmann and Ch. Herschbach, *Kunst. Plast. Euro.*, **86**, 5 (1996).
5. Z. Zhang, I. J. Britt and M. A. Tung, *J. Appl. Polym. Sci.*, **82**, 1866 (2001).
6. J. A. Wachtel, B. C. Tsai and C. J. Farrell, *J. Plast. Eng.*, **41**, 41 (1985).
7. B. C. Tsai and B. J. Jenkins, *J. Plast. Film Sheet.*, **4**, 63 (1988).
8. T. Iwanami and Y. Hirai, *Tappi J.*, **66**, 85 (1983).
9. G. W. Kamykowski, *J. Plast. Film Sheet.*, **16**, 237 (2000).
10. P. M. Subramanian, *Polym. Eng. Sci.*, **25**, 483 (1985).
11. P. M. Subramanian and V. Mehra, *Polym. Eng. Sci.*, **27**, 663 (1987).
12. S. Y. Lee and S. C. Kim, *Polym. Eng. Sci.*, **37**, 463 (1997).
13. R. Gopalakrishnan, J. M. Schultz and R. M. Gohil, *J. Appl. Polym. Sci.*, **56**, 1749 (1995).
14. M. R. Kamal, I. A. Jinnah and L. A. Utracki, *Polym. Eng. Sci.*, **24**, 1337 (1984).
15. S. Y. Lee and S. C. Kim, *J. Appl. Polym. Sci.*, **68**, 1245 (1998).
16. R. Gonzalez-Nunez, B. D. Favis, P. J. Carreau and C. Lavallee, *Polym. Eng. Sci.*, **33**, 851 (1993).
17. K. Min, J. L. White and J. F. Fellers, *Polym. Eng. Sci.*, **24**, 1327 (1984).
18. S. Wu, *Polym. Eng. Sci.*, **27**, 335 (1987).
19. J. H. Yeo, C. H. Lee, C. S. Park, K. J. Lee, J. D. Nam and S. W. Kim, *Adv. Polym. Tech.*, **20**, 191 (2001).
20. M. J. Folkes and P. S. Hope, *Polymer Blends and Alloys*, Blackie Academic & Professional, London, 1993.
21. U. Sundararaj and C. W. Macosko, *Macromolecules*, **28**, 2647 (1995).
22. R. Fayt, R. Jerome and Ph. Teyssie, *J. Polym. Sci., Polym. Phys. Ed.*, **20**, 2209 (1982).
23. C. C. Chen and J. L. White, *Polym. Eng. Sci.*, **33**, 923 (1993).
24. R. Holsti-Miettinen, J. Seppala and O. T. Ikkala, *Polym. Eng. Sci.*, **32**, 868 (1992).

25. L. E. Nielsen and R. F. Landel, *Mechanical Properties of Polymers and Composites*, Marcel Dekker, New York, 1994.
26. C. E. Scott and C. W. Macosko, *Polym. Eng. Sci.*, **35**, 1938 (1995).
27. C. W. Macosko, P. Guegan, A. K. Khandpur, A. Nakayama, P. Marechal and T. Inoue, *Macromolecules*, **29**, 5590 (1996).
28. O. T. Ikkala, R. M. Holsti-Miettinen and J. Seppala, *J. Appl. Polym. Sci.*, **49**, 1165 (1993).
29. H. S. Moon, B. K. Ryoo and J. K. Park, *J. Appl. Polym. Sci.*, **32**, 1427 (1994).
30. H. Garmabi and M. R. Kamal, *J. Plast. Film Sheet.*, **15**, 120 (1999).
31. Automatic Manometric Gas Permeability Tester Operator Manual, Model L100-5000, Lyssy AG, 2001.
32. R. Gopalakrishnan, J. M. Schultz and R. M. Gohil, *J. Appl. Polym. Sci.*, **56**, 1749 (1995).
33. G. I. Taylor, *Proc. R. Soc. London Ser. A*, **138**, 41 (1932).
34. G. I. Taylor, *Proc. R. Soc. London Ser. A*, **146**, 501 (1934).
35. F. Avalos, M. Arroyo and J. P. Vigo, *J. Polym. Eng.*, **9**, 158 (1990).
36. M. Joshi, S. N. Maiti and A. Misra, *Polym. Compos.*, **15**, 349 (1994).